Resin Pocket Enhancement through Anisotropic Diffusion

Giuseppe Parziale[a], Alfred Rinnhofer[b]

Joanneum Research
Institute of Digital Image Processing
Machine Vision Group
Wastiangasse 6, A-8010 Graz, Austria
[a] giuseppe.parziale@joanneum.at
[b] alfred.rinnhofer@joanneum.at

Abstract

The increasing demand for wood products with better defined quality parameters has led the wood industry to find improved methods for converting logs into final products. The number and the type of defects (e.g. knots, cracks, resin pockets, wane, pith, and decay) define the quality of lumber. In particular, the presence or absence of these defects determines the visual appearance, constructive strength and, in combination, the quality and price of the product. Computer Tomography (CT) can be used to inspect the internal structure of logs and to determine their interior defects before breakdown. In this paper, we present a method for the localization of resin pockets in CT images, based on anisotropic diffusion filtering. We use this filter to enhance the resin pockets edges, afterwards detected by an edge detector.

1. Introduction

The increasing demand for wood products with better defined quality parameters has led the wood industry to find improved methods for converting logs into final products. The quality of lumber is defined by the number and the type of defects (e.g. knots, cracks, resin pockets, wane, pith, and decay). In particular, the presence or absence of these defects determines the visual appearance, constructive strength and, in combination, the quality and price of the product. Moreover, Computer Tomography (CT) can be used to inspect the internal structure of logs and to determine their interior defects before breakdown. As a consequence, the defects, normally hidden inside a log, can be taken into account during saw milling, producing higher quality lumber. A complex CT image processing system is currently being developed at Joanneum Research for log defects localization. In this paper, we present only one module for defects detection: the localization of resin pockets, based on anisotropic diffusion filtering.

Multiscale image enhancement and representation is an important part of biological and machine early vision systems. In the last decade nonlinear diffusion filters have become a powerful and well-founded tool in multiscale image analysis ([1], [4], [8], [9], [13], [17], [18], [19]). These models lead to an image simplification, which simultaneously preserves or even enhances semantically important information such as edges, lines or flow-like structures. Anisotropic diffusion has already been used for image enhancement and edge detection ([2], [3], [10], [11], [14]).

2. Anisotropic Diffusion

2.1 General idea

Diffusion is a physical process equilibrating concentration differences without creating or destroying mass [9]. Fick's law [16] describes the equilibrium property of these processes:

$$(1)\quad \vec{\Phi} = -D\vec{\nabla}C = -D\vec{grad}C\,.$$

This equation states that a concentration gradient $\vec{\nabla}C$ generates a flux $\vec{\Phi}$, compensating this gradient. The quantities $\vec{\nabla}C$ and $\vec{\Phi}$ are related by the diffusion tensor D, a positive definite symmetric matrix[1]. When $\vec{\nabla}C$ and $\vec{\Phi}$ are parallel, the diffusion process is called isotropic, otherwise anisotropic. Moreover, if the diffusion tensor is constant, the diffusion process is said to be homogeneous, while in the other cases it is called inhomogeneous.
Due to the fact that during diffusion processes, mass is not created or destroyed, we can consider the continuity equation

$$(2)\quad \frac{\partial C}{\partial t} = -div\vec{\Phi}\,,$$

where t is the time and *div* is the divergence operator[2], and substituting (1) in (2), we end up with

$$(3)\quad \frac{\partial C}{\partial t} = div\left(D\vec{\nabla}C\right) = D\Delta C + \vec{\nabla}D\cdot\vec{\nabla}C$$

where Δ is the Laplacian operator[3]. This equation represents a diffusion process. In the image-processing field, we can identify the concentration $C(x,y,t)$ with the gray level $u(x,y,t)$ at a certain image location and certain diffusion time. If the tensor D is a function of the differential structure of the evolving image, the diffusion is called nonlinear; while in the other cases, it is called linear. For a complete review of the definitions of linear and non-linear, homogeneous and inhomogeneous filtering, refer to [4], [9] and [25].
Perona and Malik proposed in [1] a diffusion process, which can be seen as a special case of the diffusion equation (3). They apply an inhomogeneous process that reduces the diffusivity at those locations, which have a larger likelihood to be edges. They measure this likelihood by $|\nabla u|^2$. The Perona-Malik equation is

$$(4)\quad \frac{\partial u}{\partial t} = div\left(D(|\nabla u|^2)\vec{\nabla}u\right)$$

where

[1] The matrix $A\in\Re^{mxn}$ is positive definite, if $x^T Ax > 0$ for all non-zero vectors $x\in\Re^n$.

[2] $div\vec{F} = \frac{\partial F_x}{\partial x} + \frac{\partial F_y}{\partial y} + \frac{\partial F_z}{\partial z} = \vec{\nabla}\cdot\vec{F}$

[3] $\Delta = \vec{\nabla}\cdot\vec{\nabla} = \nabla^2 = \frac{\partial^2}{\partial x^2} + \frac{\partial^2}{\partial y^2} + \frac{\partial^2}{\partial z^2}$

$$(5)\quad D(|\nabla u|^2) = \frac{1}{1+\frac{|\nabla u|^2}{K^2}}$$

with K (contrast parameter) controlling the diffusion strength. The equation (4) is a nonlinear partial differential equation of a type that is difficult to analyze and is unstable for some parameter regimes [19].
In equation (4), image intensity is treated as a conserved quantity and allowed to diffuse over time, with the amount of diffusion at a point being inversely related to the magnitude of the intensity gradient at that location. For a better understanding of the Perona-Malik filter at the edges, let us consider the one-dimensional case. Equation (5) can be written as

$$(6)\quad g(s) = \frac{1}{1+s^2/K^2}.$$

Plotting (6) (Fig. 1) for different values of K, one can see how the function decreases for increasing values of s (gradient) and for different values of K.

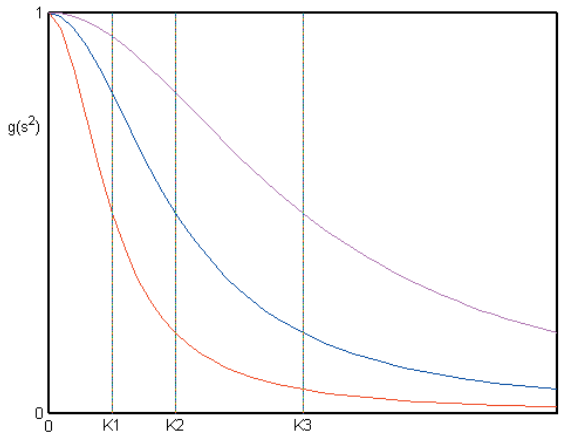

Figure 1: Diffusion parameter as a function of the image gradient.

K plays the role of a *contrast parameter* separating low contrast from high contrast diffusion areas. This means that for larger gradient values the diffusion process is soft, while for smaller gradient values (quite constant gray level) the diffusion process is stronger. In this way, edges are preserved in the image.

2.2 Numerical implementation

In [4], Weickert shows the properties and the conditions for a convergence of the numerical implementation of equation (3). We use a numerical implementation of the form

$$(7)\quad S_{i,j,t+1} = S_{i,j,t} + \lambda\left(c_N\nabla_N + c_S\nabla_S + c_E\nabla_E + c_W\nabla_W\right)$$

where $S_{i,j,t}$ is the image intensity at location (i,j) and iteration step t, λ[4] is the diffusion strength and

$$(8)\quad \begin{aligned} \nabla_N &= S_{i,j+1,t} - S_{i,j,t} \\ \nabla_S &= S_{i,j-1,t} - S_{i,j,t} \\ \nabla_E &= S_{i-1,j,t} - S_{i,j,t} \\ \nabla_W &= S_{i+1,j,t} - S_{i,j,t} \end{aligned}$$

are the numerical derivatives (differences) in the four directions and

$$(9)\quad c_x = \frac{1}{1+\frac{\nabla_x}{K}} \text{ with } x = N,S,E,W$$

are the diffusion coefficients in the four directions[5]. As one can see, if we measure a large intensity variation along one direction (presence of an edge), the coefficient c_x in that direction becomes small and the relative diffusion term in equation (7) is reduced. The gray level variation is weighted through the contrast parameter K. The entire process is iterative and the number of iteration has to be fixed as a function of the application.

3. Resin pockets

3.1 Description

Resin pockets are usually lens-shaped accumulations of liquid or solidified resin. Distribution and size of the pockets within and between trees, and between forests, are unpredictable. Their effect is the reduction of clear wood and clear cuttings yields. In Fig. 2a, 2b e 2c, some examples of resin pockets on board surfaces are shown.

3.2 Enhancement and detection

Figure 3 shows three examples of CT image details where resin pockets are highlighted. As one can see, resin pockets are represented by both high gray level values (high density resin pockets – Fig. 3a e 3b) and low gray level values (low density resin pockets – Fig. 3c).

[4] Perona and Malik suggested $0 \le \lambda \le 1/4$ for a numerical stability [1].

[5] N, S, E, W are the mnemonic subscripts for North, South, East and West.

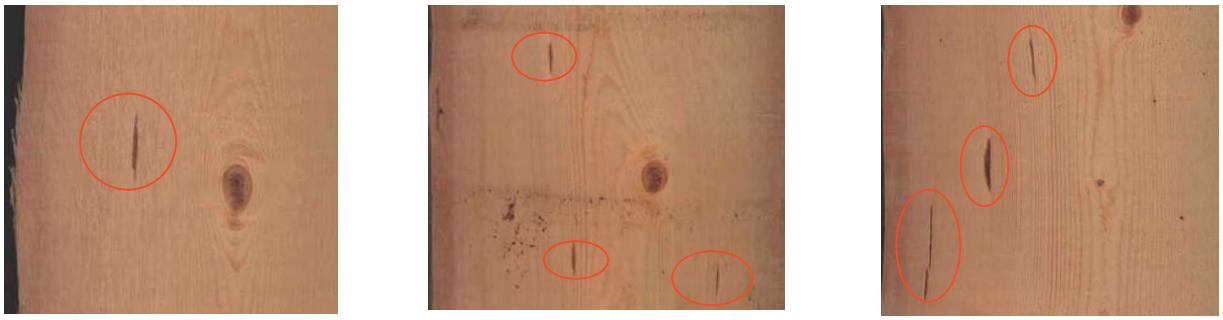

Figures 2a, 2b and 2c: Example of resin pockets on the board surfaces after the cut.

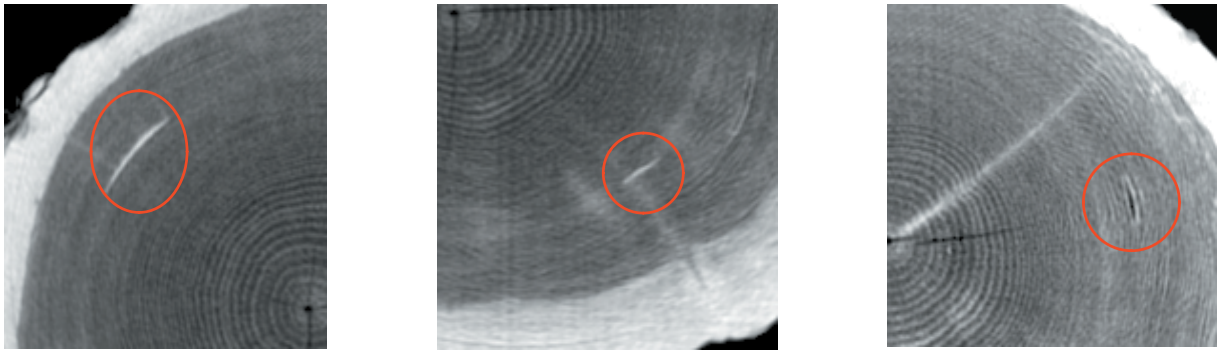

Figures 3a, 3b and 3c: Examples of resin pockets in CT images.

The idea of the algorithm is to look for the resin pocket bounds applying an edge detector on the image. However, due to the poor quality of images coming from industrial CT scanners [20], the direct application of an edge detector on the original image leads us to a very noisy result. This is shown, for example, in Fig. 5, where the image represents the edges extracted by the edge detector [22] from the image of Fig. 4. As one can see, edges belonging to the annual rings, the separation surface between heartwood and sapwood, the cracks, the resin pockets and the knots[6] have been detected. The extrapolation of the resin pocket edges (signal) from the other ones (noise) is very difficult at this processing step. Thus, an enhancement of the resin pocket edges and a reduction of other edges are required. This is easily achievable through the anisotropic diffusion filtering.

In general, the target of filtering an image is to exchange the intensity value at each pixel through some linear or nonlinear function of its near neighbors, with the scope of producing a pixel value which is more representative of the region in which it lies. However, pixel values that lie on the border of two regions are not representative of either, but rather of some intermediate value [21]. In this case, it has to be estimated if a pixel belongs to an edge or to an interior region. For each image pixel, we measure this probability through equation (9) and compute the new gray level value using equation (7).

[6] This image (Fig. 4) doesn't contain knots, but, when they are present, their edges appear in the result image.

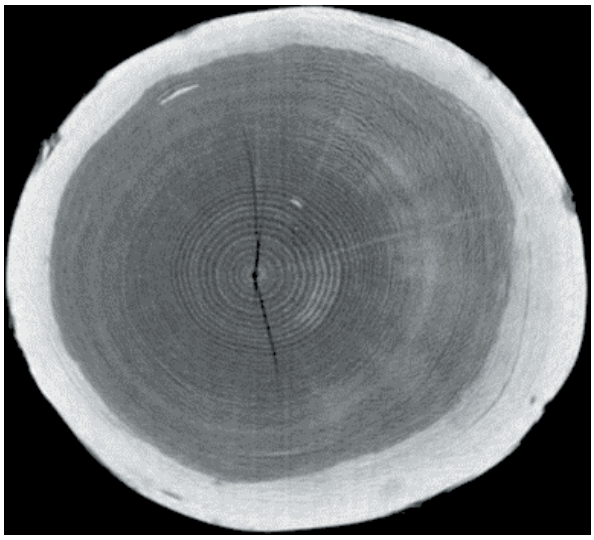

Figure 4. Original image

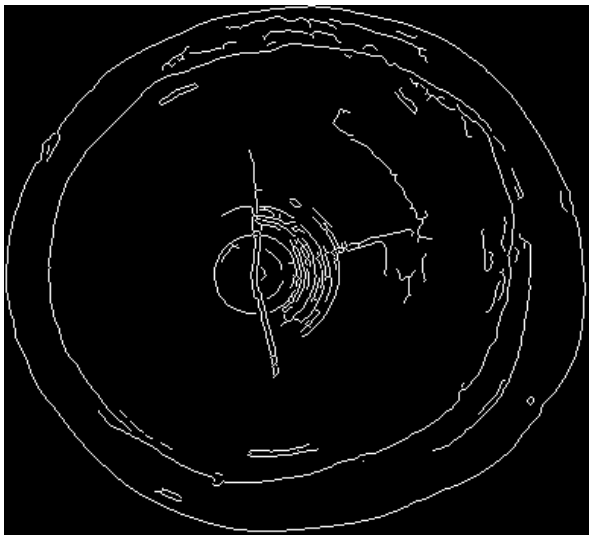

Figure 5. Detected edges of the original image

Fig. 6 shows the result of the anisotropic diffusion filter applied on the original image (Fig. 4). As one can see, the resin pockets and the cracks are still visible, while the annual rings have been completely diffused. Applying the edge detector at this step, we end up with the result in Fig. 7. Here, the resin pockets bounds are still visible.

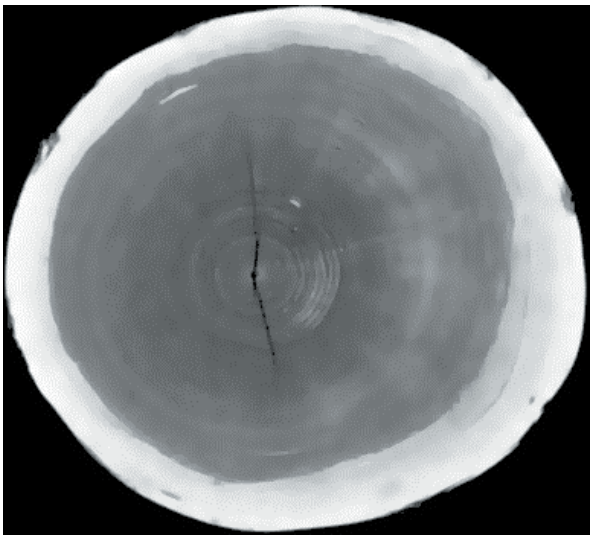

Figure 6. Result of anisotropic diffusion filter

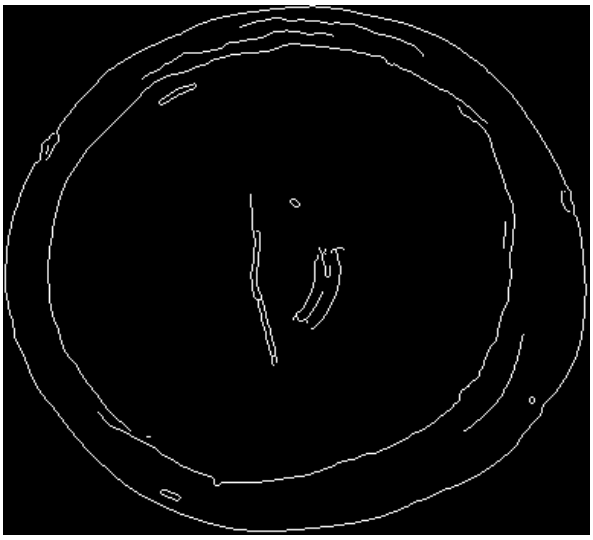

Figure 7. Detected edges after anisotropic diffusion filter

The separation of the resin pocket edges from edges belonging to other defects is easy at this point. While knots and cracks are radial with respect to the log, resin pockets are longitudinal. This *a-priori* knowledge helps us to easily separate these defects with the blob analysis (Fig. 9).

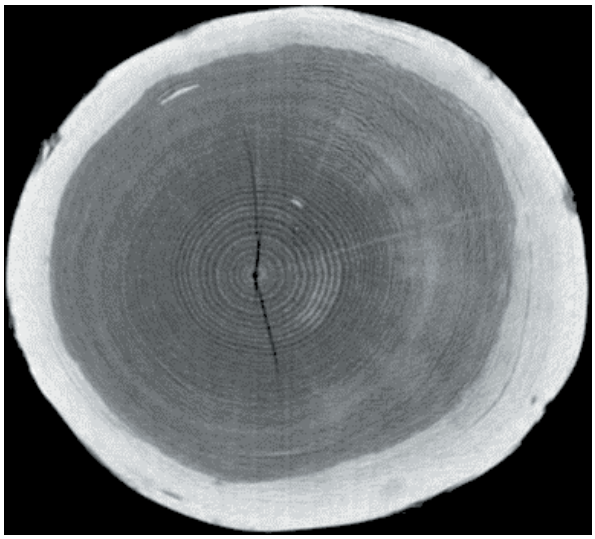

Fig. 8. Original image (reported again here for an easy comparison with the result)

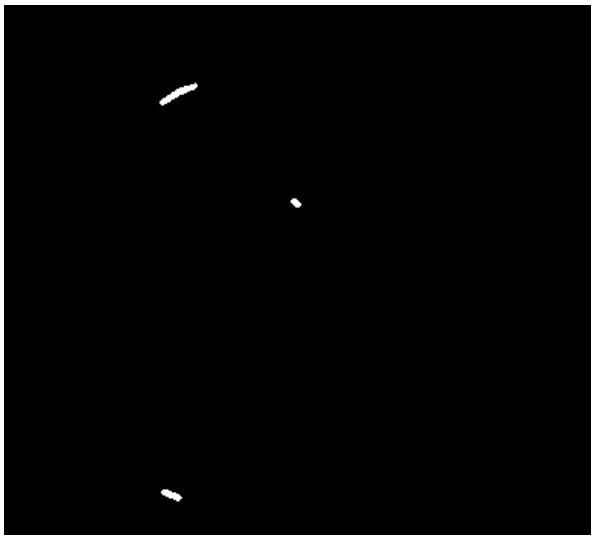

Fig. 9. Final result: complete detection

4. Results and discussion

Analyzing equations (7) and (9), we find out that, before the application of anisotropic diffusion, the number of iteration N, the contrast parameter K and the diffusion strength λ have to be fixed. We will refer to K and λ as *structural parameters* and to N as *temporal parameter*.

The structural parameters have to be chosen according to the size of the structures that have to be enhanced. The value of K has to be chosen, as it was explained in the paragraph 2.1. In our case, we have observed that resin pockets could have a variable length, but a width of at least 4 pixels. Our experiments lead us to choose a value $K = 20$. Moreover, as suggested in [1], the diffusion strength value has to be $0 \le \lambda \le 1/4$, ensuring the numerical convergence.

From a computation-time point of view, the temporal parameter N is the most critical. The larger the iteration number one chooses, the stronger the edge enhancement[7] and the bigger the computation time it is. We chose a value of 30 iterations (N=30). In this way, we observed a good noise reduction and an acceptable computational time. The algorithm was implemented in C++ and executed on a double Pentium IV with 2.2 GHz and 512 GByte of DDRAM. On this system, the 30 iterations needed 3 s and the total resin pocket detection (anisotropic diffusion, edge detection, blob analysis) needed 5 s. This result is still far from the target computational time we want to achieve on the complete system[8].

In the literature, many solutions have been proposed ([5], [6], [7], [12], [15], [21], [23], [24]) for the time improvement of the anisotropic diffusion and we are experimenting some of them. Our studies and researches are mainly in the direction of the bilateral filters that represent a valid alternative to the anisotropic diffusion filtering in terms of time performances and results.

Regarding the detection rate, it has to be outlined that, because of the limited resolution, sometimes it is not easy, even for an expert, to detect resin pockets in the CT images. In the sapwood, due to humidity changes, some structures with the same density and shape of the resin pockets are present

[7] In reality, an upper limit for N exists: a number of iterations bigger than 300 would lead to a completely diffused image, where only the sapwood and heartwood are visible.

[8] The final system should be able to process all the defects in 1 second for each image. This is because an industrial CT scanner can deliver images with a speed of 1 image/s.

(Fig. 4) and this leads us to an objective difficulty in their identification. Moreover, in the heartwood, it is almost impossible to see low-density resin pockets. In order to compare the algorithm results and the real resin pocket localization, we had to cut a log and verify the detection rate.

5. Summary

In this paper, we have presented an algorithm for resin pocket enhancement in images coming from industrial CT scanners. The idea is to detect resin pockets edges, but, because of the limited resolution of images produced by industrial CT scanners, we need to enhance them. We have used nonlinear anisotropic diffusion filtering that produces uniform areas on locations where small gray level variations are present. In this way, edges result enhanced. Afterwards, an edge detector is applied and the result presents less noise than the case without anisotropic diffusion.

Acknowledgments

The authors would like to take this opportunity to thank Kurt Tschabuschnig for his help in timing analysis, benchmarking and profiling of the algorithm for the MATROX Image Library.

References

[1] P. Perona, J: Malik, Scale-Space and Edge Detection Using Anisotropic Diffusion*, IEEE Trans. Pattern. Anal. Mach. Intell*., 12, 1990, pp. 629-639.

[2] J. Weickert, Anisotropic Diffusion Filters for Image Processing Based Quality Control, *Proc. Seventh European Conf. On Mathematics in Industry*, Teubner, Stuttgart, pp. 355-362, 1994.

[3] J. Weickert, Coherence-Enhancing Diffusion Filtering, *Intern. Journal of Computer Vision*, 31, pp. 111-127, 1999.

[4] J. Weickert, Anisotropic Diffusion in image processing, in Teubner-Verlag, 1998.

[5] B. Fischl, E. Schwartz, Learning an Integral Approximation to Nonlinear Anisotropic Diffusion in Image Processing, *IEEE Trans. Pattern. Anal. Mach. Intell*., vol. 19, no. 4, 1997, pp. 342-352.

[6] J. Monteil, A. Beghdadi, A New Interpretation and Improvement of the Nonlinear Anisotropic Diffusion for Image Enhancement, *IEEE Trans. Pattern. Anal. Mach. Intell*., vol. 21, no. 9, 1999, pp. 940-948.

[7] Y. P. Wang, R. Qu, Fast Implementation of Scale-space by Interpolatory Subdivision Scheme, *IEEE Trans. Pattern. Anal. Mach. Intell*., vol. 21, no 9, 1999, pp. 933-939.

[8] J. Weickert, Scale-Space Properties of Nonlinear Diffusion Filtering with a Diffusion Tensor, Report No 110, Laboratory of Technomathematics, University of Kaiserlautern, Kaiserlautern, Germany, Oct. 1994.

[9] J. Weickert, A Review of Nonlinear Diffusion Filtering, in *B. ter H. Romeny, L. Florack, j: Koendrink, M. Viergever (Eds.), Scale-Space Theory in Computer Vision, Lecture Notes in Computer Science*, Vol. 1252, Springer, Berlin, pp. 3-28, 1997, Invited paper.

[10] M. J. Black, G. Sapiro, D. H. Marimont, D. Heeger, Robust Anisotropic Diffusion, *IEEE Trans. on Image Processing*, Vol. 7, No. 3, March 1998.

[11] K. Deguchi, T. Izumitani, H. Hontani, Detection and enhancement of line structues in an image by anisotropic diffusion, *Pattern Recognition Letters*, 23, 2002, pp. 1399-1405.

[12] M. Elad, On the Origin of the Bilateral Filter and Ways to Improve It, *IEEE Trans, on Image Processing*, vol. 11, no. 10, oct. 2002, pp. 1141-1151.

[13] H. Scharr, J. Weickert, An Anisotropic Diffusion Algorithm with Optimized Rotation Invariance, in *G. Sommer, N. Krüger, Ch. Perwass (Eds.), Mustererkennung 2000*, Springer, Berlin, pp. 460-467, 2000.

[14] A. Fco. Solé, A. López, G. Sapiro, Crease Enhancement Diffusion, *Computer Vision and Image Understanding*, 84, 241-248, 2001.

[15] C. Tomasi, R. Manduchi, Bilateral Filtering for Gray and Color Images, *Proc. IEEE Intern. Conference on Computer Vision, Bombay, India, 1998.*

[16] G. L. Flynn, Mass transport phenomena and models: Theoretical concepts, *J. Pharm. Sci.*, 63, 1974, pp. 479-510.

[17] A. P. Witkin, Scale-space filtering, in *Proc. International Joint Conference on Artificial Intelligence*, pp. 1019-1021, 1983.

[18]G. W. Wei, Generalized Perona-Malik Equation for Image Restoration, *IEEE Signal Processing Letters*, vol. 6, no. 7, Jul. 1999.

[19] P. Perona, T. Shiota, J. Malik, Anisotropic diffusion, In Romeny, B. M. T. H. (ed.), Geometry Driven Diffusion in Computer Vision, Computational Imaging and Vision, chap. 3, pp. 73-92, 1994, Kluwer.
[20] J. Ph. Andreu, A. Rinnhofer, Enhancement of annual rings on industrial CT images of logs, *Proc. ICPR2002*, vol. 3, 2002, pp 261-264.
[21] B. Fischl, E. Schwartz, Adaptive Nonlocal Filtering: A Fast Alternative to Anisotropic Diffusion for Image Enhancement, *IEEE Trans. Pattern. Anal. Mach. Intell.*, vol 21, no. 1, 1999, pp. 42-48.
[22] J. Canny, A Computational Approach to Edge Detection, *IEEE Trans. on PAMI*, vol. 8, pp. 679-714, 1986.
[23] D. Barash, Bilateral Filtering and Anisotropic Diffusion: Towards a Unified Viewpoint, HP Laboratories Israel, Aug. 2000.
[24] F. Durand, J. Dorsey, Fast Bilateral Filtering for the Display of High-Dynamic-Range Images, SIGGRAPH 2002, Jul. 2002, St. Antonio.
[25] T. Lindeberg, Scale-Space: A framework for handling image structures at multiple scales, *Proc. CERN School of Computing*, Egmond aan Zeem The Netherlands, 8-21 Sept. 1996.

Giuseppe Parziale, Alfred Rinnhofer